ABSTRACT

WEINHOFER, ALISHA MARIE. Progress Towards the Total Syntheses of Bisleuconothine, Development of an Asymmetric Cyclopropanation, and Synthesis of Dual JAK/TRPV1 Inhibitors. (Under the direction of Dr. Joshua G. Pierce).

The Pierce group is interested in the study and the development of novel approaches to synthesize biologically active complex natural products. Collectively, these projects are focused on advancing total synthesis, synthetic chemistry, chemical biology, and drug discovery.

Herein, three projects are described which reflect the Pierce groups' areas of focus. The first being the synthesis of the bisleuconothines, a family of recently isolated natural products that have been reported to have promising biological activity against cancer cell lines. Second, a novel method to cyclopropanate enecarbamate containing molecules to form the privileged C3 all-carbon quaternary center featured in multiple natural product scaffolds. Lastly, the development of a novel dual JAK/TRPV1 inhibitor for the regulation of pain as a potential pharmaceutical lead.

Progress Towards the Total Syntheses of Bisleuconothine, Development of an Asymmetric Cyclopropanation, and Synthesis of Dual JAK/TRPV1 Inhibitors

By
Alisha Marie Weinhofer

A thesis submitted to the Graduate School of
North Carolina State University
in partial fulfillment of the
requirements for the degree of
Master of Science

Chemistry

Raleigh, North Carolina
2023

APPROVED BY:

_____	_____
Dr. Joshua G. Pierce	Dr. Carolina Proulx
Chair of Advisory Committee	

_____

Dr. Wei-Chen Chang

DEDICATION

This work is dedicated to my parents, Joseph and Linda, and my brother Joseph Jr. for always supporting me.

BIOGRAPHY

Alisha Maire Weinhofer was born on November 2nd, 1997 in New London, CT to Joseph and Linda Weinhofer. She was raised in Hampstead, North Carolina along with her two older brothers. Alisha graduated Topsail High School with honors in May 2015, with the knowledge that she wanted to pursue a degree in science. She went on to get her Bachelor of Science from Campbell University where during her time there she was trained in chemistry research under the advisement of Dr. Sarah Goforth. In the summer of 2017, she attended her first Research Experience for Undergraduates at Furman University under co-advisement of Dr. Brian Guess. During this time, she helped develop a novel method to synthesize silyl esters from silyl ethers. In 2019 she graduated from undergraduate and got accepted into North Carolina State University where she joined the Pierce group in the fall. During her studies she focused on the synthesis of natural products for biological evaluation.

ACKNOWLEDGEMENTS

Although this degree has only my name on it, it wouldn't have been possible without all the wonderful people in my life. Without them this journey wouldn't have been possible. Starting with my family who has supported me throughout my life and gave me the means to be who I am today.

I want to thank Dr. Houston Cole for his friendship, guidance, and encouragement throughout my journey. I wouldn't be here today if it wasn't for me seeing the immense joy you had when explaining your research to me and asking if I'd like to be apart of it.

I want to thank my undergraduate research advisor Dr. Sarah Goforth for her incredible mentorship; her enthusiasm for research plus her passion to help others grow set me up to be a good chemist.

I want to thank Amanda Ritz for her friendship, support, and advise over the years. You always had a way of calling me right when I needed to talk.

I also want to thank Carlos and Cami for their friendship, positivity, and encouragement which made this program full of fun and laughter with our many board game nights.

I would like to thank my three cats Aerith, Barrett, and Tifa for their comfort and entertainment. They have kept me going to make a better life for them.

I also want to thank everyone in the Pierce group, past and present, for laying the foundation for me to succeed. In particular I would also like to thank Alejandro Valdes for his comradery, knowledge, understanding, friendship, and insight. He made lab better even on the worst days and I will never regret picking you up in the pouring rain.

I want to thank Ivan Cockman for his love, support, partnership, trust, and friendship. Your patience, understanding, and encouragement throughout this journey gave me the courage to pursue my passions.

Last, but not least, I want to thank Dr. Joshua Pierce for the opportunity to work in his lab and grow alongside my peers. Your mentorship has led me to where I am today; I have learned so much during my time here and it is all because of the opportunity you gave me, thank you.

TABLE OF CONTENTS

LIST OF FIGURES

LIST OF TABLES

LIST OF SCHEMES

LIST OF ABBREVIATIONS

ACN: acetonitrile

AzaBOX: aza-bis(oxazoline)

Boc: tert-butyloxycarbonyl

BOX: bisoxazoline

^{n}BuLi: *n*-butyllithium

cat.: catalyst

Cbz: carboxybenzyl

DCE: 1,2-dichloroethane

DIPEA: diisopropylethylamine

DMAP: 4-dimethylaminopyridine

DMF: dimethylformamide

DMSO: dimethyl sulfoxide

DMTMM: 4-(4,6-Dimethoxy-1,3,5-triazin-2-yl)-4-methylmorpholinium chloride

EDA: ethyldiazoacetate

ee: enantiomeric excess

Et: ethyl

equiv: equivalent

LC-MS: liquid chromatography mass spectrometry

LDA: lithium diisopropyl amide

Me: methyl

MIC: minimum inhibitory concentration

min: minute

NMM: N-Methylmorpholine

NMR: nuclear magnetic resonance

OD_{600}: optical density at 600 nm (absorbance)

OTf: triflate

PG: protecting group

Pr: propyl

PTLC: preparative thick layer chromatography

rt: room temperature

rxn: reaction

S_N2: nucleophilic substitution

TBS: *tert*-butyldimethylsilyl

TFA: trifluoroacetic acid

THF: tetrahydrofuran

TLC: thin layer chromatography

Ts: tosyl

PTSA: *p*-toluenesulfonic acid

Chapter 1: Progress Towards the Synthesis of Bisleuconothine

1.1 Introduction

Cancer has been around in humans and animals from the earliest records of human history. This is an ancient disease that still plagues us till this day.[1] In 2018 the United States had 1,708,921 new cases of cancer reported and 599,265 people died of cancer.[2] In other words, for every 100,000 people, 436 new cancer cases were reported and 149 people died of cancer. This is far from where we'd like to be; however, great health care and therapeutic improvements have been made throughout history due in large part to natural products.

Natural products are the main source of small molecule cancer therapeutics most infamously represented by camptothecin and taxol.[3] In addition to these specific cancer therapeutics multiple classes have also been discovered such as camptothecins, taxanes, and rapamycin mTOR inhibitors to name a few.[4] Most of the early studies on these cancer therapeutics were through their shocking antitumor activity reported from phenotypic assays. These discoveries lead to major pharmaceutical companies funding the discovery of novel natural products for drug leads primarily from the 1950s to the beginning of the 1980s. During the beginning of the 1980s there was a switch to process-based target-driven drug discovery such as high-throughput screening of synthetic compounds or natural product derivatives. These methods were thought to be good for understanding small molecule mechanisms and rapidly discover potential therapeutics. These approaches were also initiated due to the decline in novel natural product scaffolds being discovered. Now, many major pharmaceutical companies are no longer relying on natural product-based drug discovery but instead this area of research is being relegated to academic groups.

With a decreased pharma presence, there is still a need to discover novel natural products for their innate bioactive characteristics. Since 1981 to 2019 approximately 25% of all newly approved anti-cancer drugs were derived from natural products.[3] Natural products also allow for the advancement of synthetic chemistry though the synthetic development toward these complex molecules. Therefore, natural products are still of interest as cancer drug leads and are important for the development of innovative and broadly useful synthetic methods.

1.1.1 Isolation of bisleuconothine

Bisleuconothines A-D are a new family of bisindole alkaloids that have been isolated from the bark of a tropical plant found on the coast of Indonesia and Malaysia called *Leuconotis griffithii*.[5,6] Bisleuconothine A and C are of particular interest because of their unique structural skeletons which consist

of eburnane-aspidospermadine and melokhanine E-aspidospermadine, respectively, linked together with a single C-C bond (**Figure 1**).

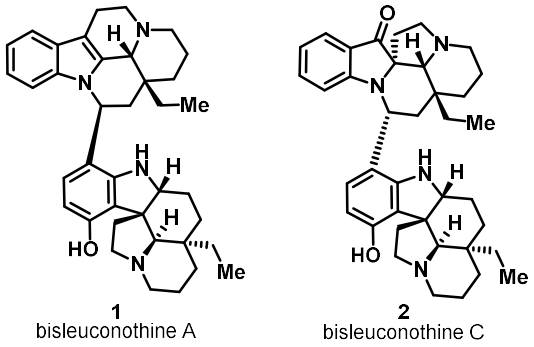

Figure 1. Bisleuconothine A and C

Both bisleuconothine A and C were tested against the human cancer cell line A549 to determine their cell growth inhibitory concentration (**Table 1**).[5,6] Bisleuconothine A was found to show cytostatic activity for A549, which was also the case when tested against HL60, HCT116, and MCF7 cancer cell lines.

Table 1. Reported inhibitory concentrations for bisleuconothine A and C for various human cancer cell lines

human cancer cell lines	IC_{50} values (μM)	
	bis A	bis C
HL60	11.0	---
HCT116	5.7	---
MCF7	9.2	---
A549	7.0	> 10

1.1.2 Mode of action of bisleuconothine A

Bisleuconothine A (**1**) was further studied to determine the mode of action in the A549 human cancer cell line.[7] It was determined that bisleuconothine A was able to induce autophagosome formation via a phosphorylation cascade that inhibited the AKT-mTOR signaling pathway (**Scheme 1**). Many autophagy-inducing compounds tend to induce apoptosis which is undesirable as it can contribute to the spread of cancer to other cells. However, bisleuconothine A was found to not induce apoptosis even at high concentrations, making it a good potential anti-cancer drug worth exploring.

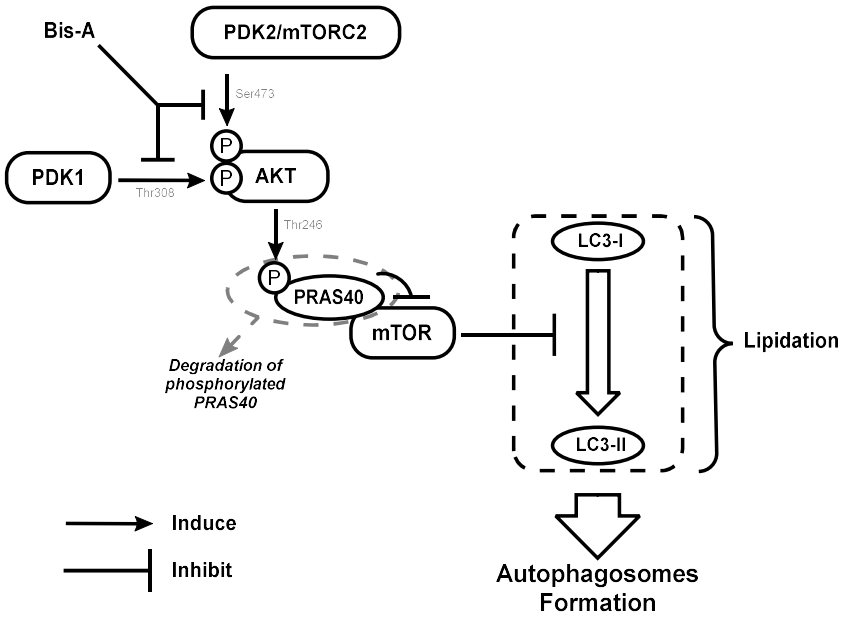

Scheme 1. Bisleuconothine A's effect on the AKT-mTOR pathway

1.2 Synthetic strategy

Bisleuconothine A and C are both structurally complex and have innate biological activity making them a primary candidate for the Pierce group's goal of synthesizing complex natural products with the potential for drug development. When comparing the two structures, by removing the C-C bond connecting the two subunits it can be identified that bisleuconothine A and C are composed of two smaller complex natural product derivatives (**Scheme 2**). Eburnamonine, melokhanine E, and aspidospermidine make up bisleuconothine A and C with aspidospermidine being a shared fragment between the two compounds.

Eburnamonine **3**, an eburane alkaloid, is reported to have potent antibacterial activity and preventative effects against cerebrovascular disorders.[8] Melokhanine E **5**, is reported to exhibit antibacterial activity and aspidospermidine **4** being a member of the monoterpene indole alkaloid family, has long been used for traditional medicine.[9,10] All three of these natural products have been synthesized over the years and melokhanine E was previously synthesized in the Pierce lab.[11]

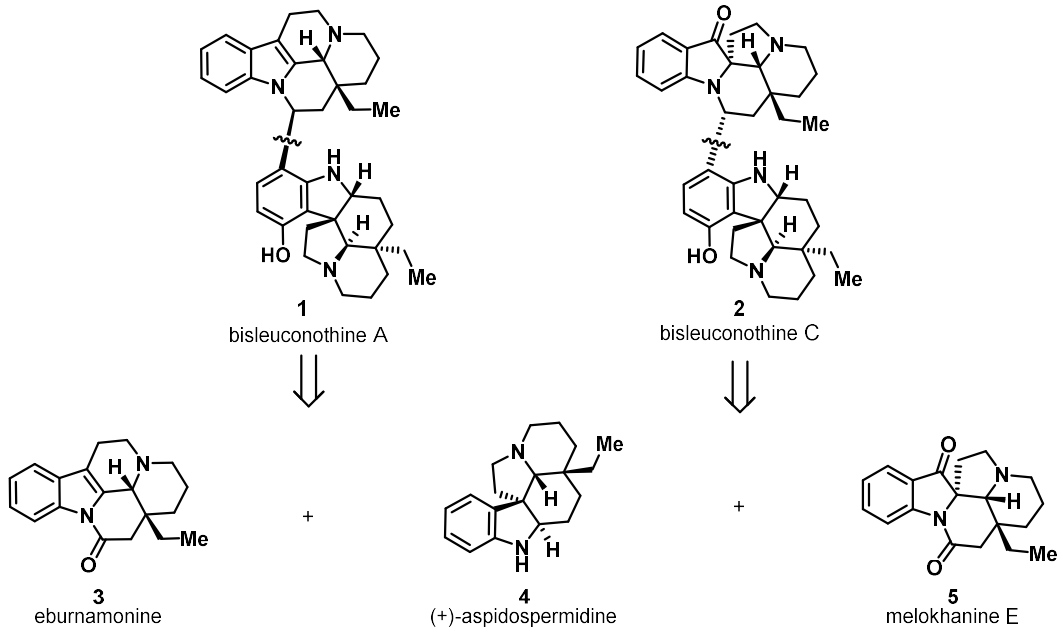

Scheme 2. Retrosynthetic analysis of bisleuconothine A and C

1.2.1 Melokhanine E synthesis

A stereocontrolled synthesis of (±)-melokhanine E (**5**) was previously developed by the Pierce group via an intramolecular formal [3 +2] cycloaddition (**Scheme 3**). This method utilized the 1,3-dipole formed from a MgI_2 catalyzed cyclopropane opening to embed all relative stereochemistry in a single transformation. This is made possible by the thermolysis of the Boc group in the microwave, thereby forming an imine. To make the biscyclopropane **7** precursor, an amine coupling was employed via the spirocyclic indolinone **8** and the carboxylic acid **9**.

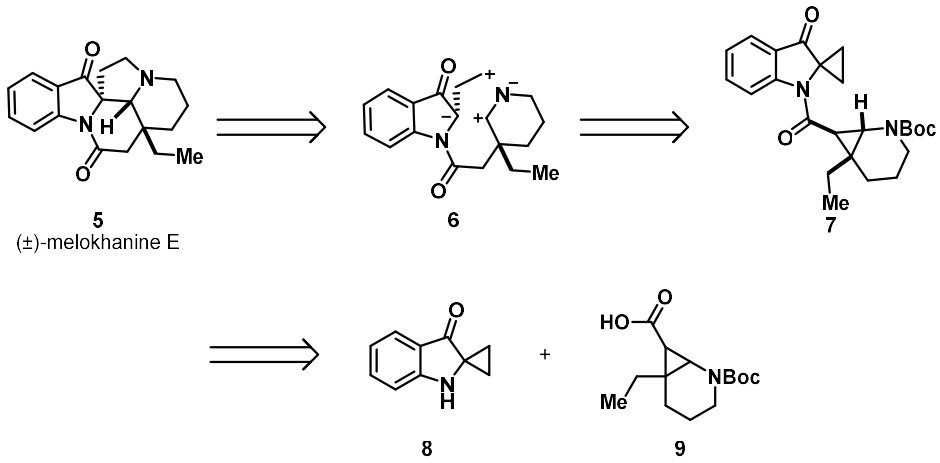

Scheme 3. Retrosynthetic strategy to access melokhanine E

To access the spirocyclic indolinone **8**, anthranilic acid **10** was reacted with bromo-lactone **12** to yield the amino acid **13** (**Scheme 4**). The carboxylic acid **13** was then activated in the presence of base to forge the spirocyclic bicycle **14**. A Krapcho decarboxylation-ring contraction was then performed in the presence of heat and NaCl to form an alpha-keto cyclopropane **15**. Lastly, the acyl group was removed via methanolysis to give the desired spirocyclic indolinone **8** precursor.

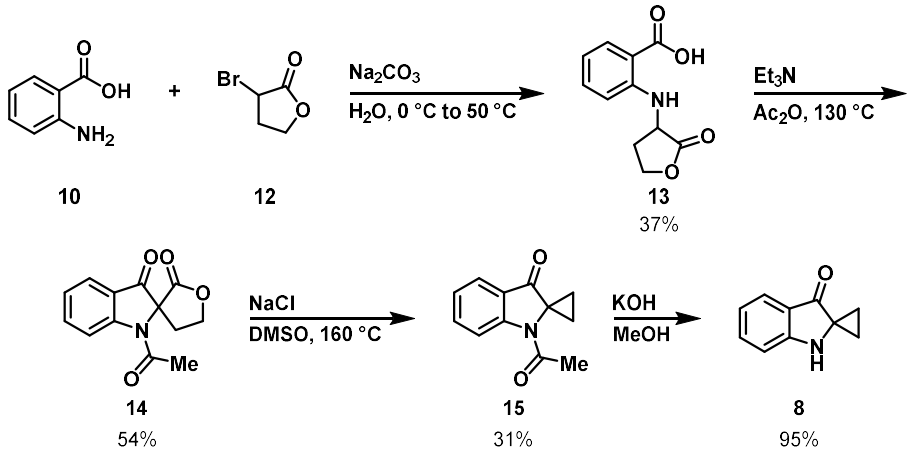

Scheme 4. Spirocyclic indolinone synthesis.

To access the carboxylic acid cyclopropane piperidine **9**, delta-valerolactam (**16**) was treated with 2.0 equivalents of *n*-BuLi and the resulting dianion was alkylated with EtI to generate **17** (**Scheme 5**). Next the amine was protected, in this case as the benzylcarbamate instead of the original tert-butylcarbamate to act as a uv-handle, to form **18**. The protected ethyl lactam **18** then underwent a reduction in the presence of $NaBH_4$ to form the alcohol then eliminated with acid to form the enecarbamate **19**. A copper(I) triflate mediated cyclopropanation of the enecarbamate **19** afforded the fused ester cyclopropane **20**, which was finally saponified under basic conditions to form the desired carboxylic acid **9**.

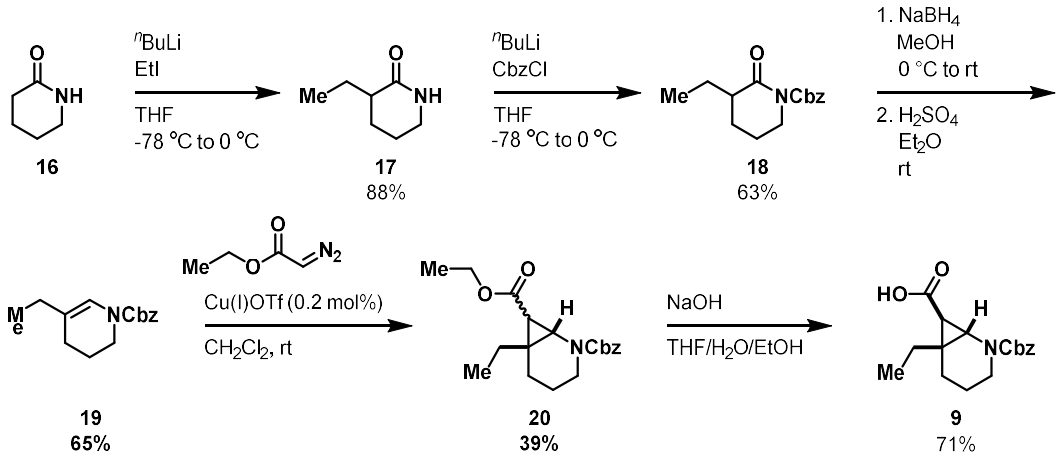

Scheme 5. Carboxylic acid containing piperidine synthesis.

With both coupling partners in hand, **8** and **9** were linked together through an amide coupling facilitated by BTC and collidine to yield the coupled product **21** (**Scheme 6**). The final step executes the key step for this synthesis involving the intramolecular [3 + 2] facilitated by MgI_2 under microwave conditions to yield (±)-melokhanine E (**5**).

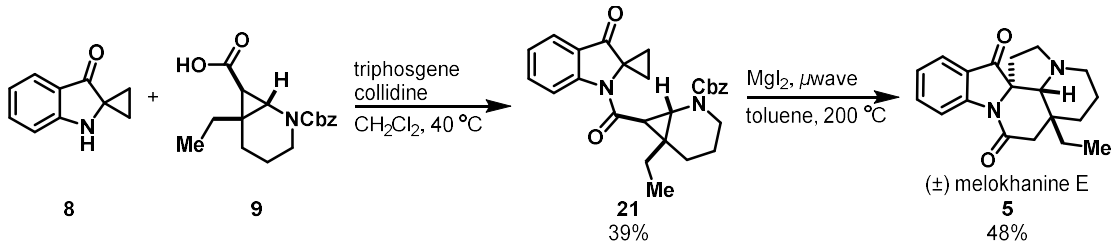

8 9 **21** 39% **5** 48%

Scheme 6. Amide coupling and the intramolecular formal [3 + 2] cycloaddition.

1.2.2 Eburnamonine synthesis

There are currently a few different published methods to synthesize eburnamonine **3**.[12,13] However, the method published by Zhu and coworkers utilizes the direct conversion of (±)-melokhanine E (**5**) to the target (±)-eburnamonine (**3**) via a chemoselective reduction followed by a simple aza-pinacol rearrangement under acidic conditions (**Scheme 7**).[8] The Zhu total synthesis of (±)-eburnamonine **3** is a total of 15 steps but if using our method to access (±)-melokhanine E (**5**) the final step count would be 13.

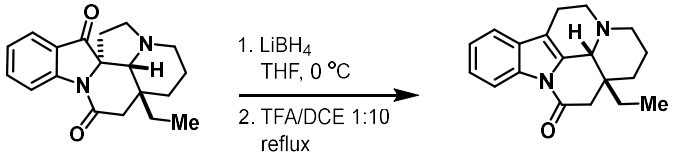

(±) melokhanine E **5** (±)-eburnamonine **3**

Scheme 7. Synthesis of (±)-eburnamonine.

1.2.3 Aspidospermidine synthesis

Similarly, to eburnamonine (**3**), there are multiple published methods for the synthesis of aspidospermidine (**4**). However, the alcohol substituted form of aspidospermidine is needed to make our target molecules bisleuconothine A and C; this derivative will be called 9-aspidospermidinol (**29**). The formal synthesis for aspidospermidine **4** was published by the Waser group and is the inspiration for our synthesis of melokhanine E **5**.[14] The two syntheses follow the same route up until the formation of the carboxylic acid cyclopropane **9** (**Scheme 8**). Starting from the carboxylic acid cyclopropane **9**, 4-(4,6-dimethoxy-1,3,5-triazin-2-yl)methylmorpholinium (DMTMM) and *N*-methyl-morpholine (NMM) were introduced to convert **9** into the Weinreb amide **22**. The Weinreb amide would then be coupled with the *N*-carboxy indole **32** to yield the homo-Nazarov precursor **23**. A homo-Nazarov cyclization could then be conducted on **23** using $Cu(OTf)_2$ to catalyze the C3 indole ring cyclization and form **24**. Deprotection of **24**

would leave the free amine **25** and concludes Waser's formal synthesis of aspidospermidine as a similar intermediate to **25** has been reported by Wekert and Hudlicky's synthesis of aspidospermidine.[12]

Once the free amine **25** is in hand, a reduction of the ketone to form **26** will be performed. Then **26** will be subjected to ethylene bromide and potassium carbonate to form the pyrrolidine **27**. A reduction of **27** would generate the free amine **28** and finally a deprotection of the alcohol would provide the target molecule aspidospermidinol **29**.

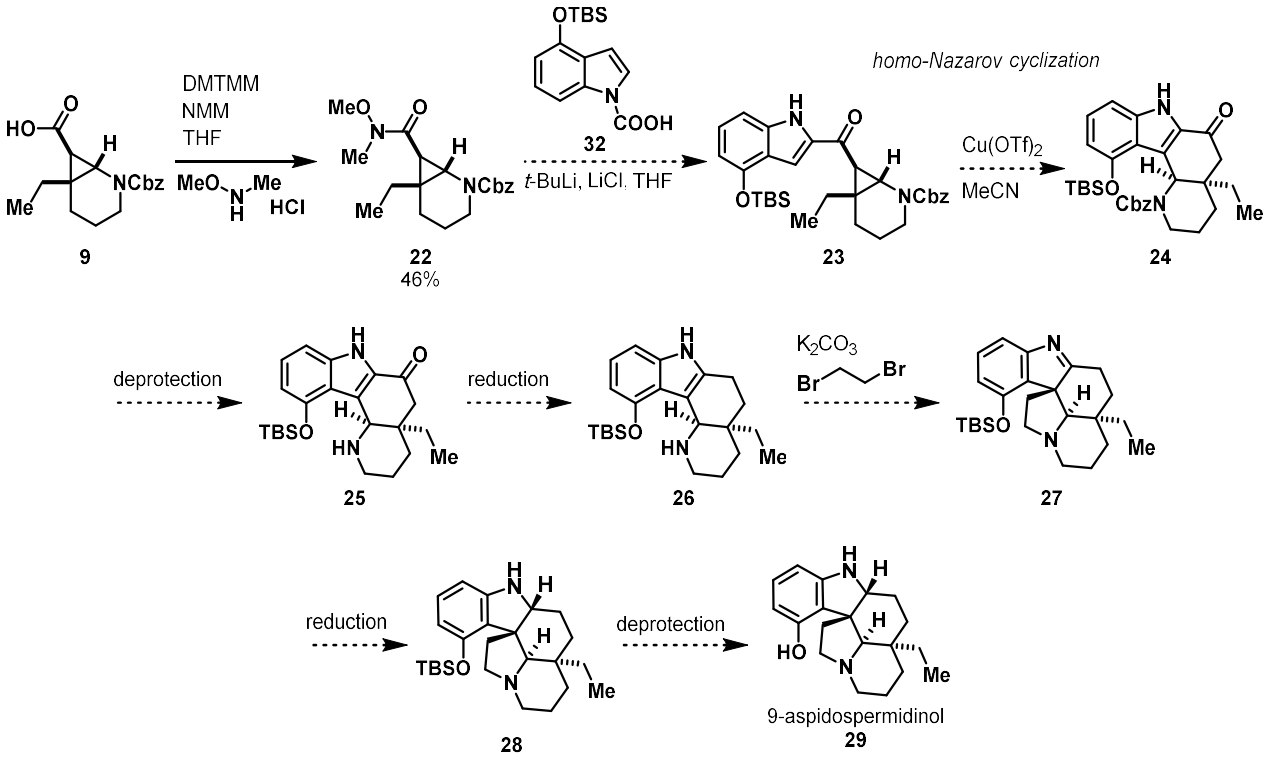

Scheme 8. Proposed aspidospermidinol synthesis.

To make the *N*-carboxy indole coupling partner **32**, 4-hydroxyindole **30** was protected with *tert*-butyl(dimethyl)silyl (TBS) to yield **31** which was then treated with ^{n}BuLi and CO_2 gas to give the *N*-carboxy indole coupling partner **32** (**Scheme 9**).

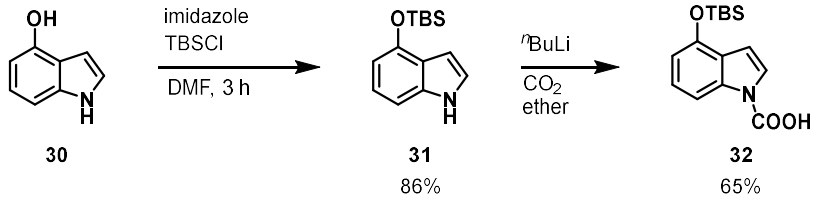

Scheme 9. *N*-carboxyl indole coupling partner for aspidospermidinol synthesis.

1.3 Conclusions and future directions

Herein, I've outlined the current synthetic progress towards the total synthesis of bisleuconothines A and C. Melokhanine E has been accessed utilizing an intramolecular formal [3 + 2] cycloaddition. Eburnamonine can be easily obtained from the direct conversion of melokhanine E via an aza-pinacol rearrangement. Efforts to complete the shared coupling partner between aspidospermidine are underway utilizing a modified version of a published formal synthesis.

Once both the top and bottom fragments of bisleuconothine A and C are in hand a series of conditions will be screened to determine the functionality of each fragment and to determine potential coupling conditions. Currently the method mentioned here would not yield an asymmetric product. However, by rendering the shared cyclopropane piperidine moiety **9** asymmetric, early in the synthesis during the cyclopropanation step, will set the final stereochemistry for the rest of the synthesis. This will be discussed in the next chapter.

1.4 Experimental

General: THF and dichloromethane were purified using an alumina filtration system. Starting materials were purchased from a commercial chemical company and used as received. Reactions were monitored by TLC analysis (pre-coated silica gel 60 F254 plates, 250 mm layer thickness) and visualization was accomplished with a 254 nm UV light and silica iodine chamber. Reactions were also monitored by LC-MS (2.6 mm C18 50 x 2.10 mm column). Flash chromatography on SiO_2 was used to purify the crude reaction mixtures and performed on a flash system utilizing pre-packed cartridges and linear gradients. ^{1}H and ^{13}C NMR spectra were obtained on a 500 or 600 MHz instrument in $CDCl_3$ or acetone-d_6 unless otherwise noted. Chemical shifts were reported in parts per million with the residual solvent peak used as an internal standard ($CDCl_3$ = 7.26 ppm for ^{1}H and 77.16 ppm for ^{13}C, acetone-d_6 = 2.05 ppm for ^{1}H and 29.84 ppm for ^{13}C NMR). ^{1}H NMR spectra were run at 500 or 600 MHz and are tabulated as follows: chemical shift, multiplicity (s = singlet, d = doublet, t = triplet, m = multiplet, bs = broad singlet, dd = doublet of doublets), number of protons, and coupling constant(s). ^{13}C NMR spectra were run at, 125 MHz or 175 MHz using a proton-decoupled pulse sequence with a d1 of 1 second unless otherwise noted and are tabulated by observed peak. High-resolution mass spectra were obtained on an ion trap mass spectrometer using heated electrospray ionization (HESI).

Compounds **5**, **8**-**9**, **13**-**15**, and **17**-**22** were prepared by known literature methods.[11,14,15]

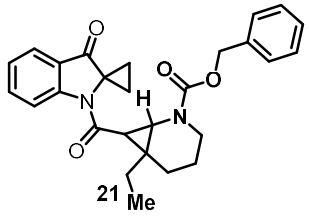

Benzyl 6-ethyl-7-(3'-oxospiro[cyclopropane-1,2'-indoline]-1'-carbonyl)-2-azabicyclo[4.1.0]heptane-2-carboxylate (21).[11] A round bottom flask and magnetic stir bar were flame-dried and placed under N_2 atmosphere. 2-(*tert*-butoxycarbonyl)-6-ethyl-2-azabicyclo[4.1.0]heptane-7-carboxylic acid (0.10 g, 0.33 mmol, 1.0 equiv), CH_2Cl_2 (3.3 mL, 0.1 M) and BTC (0.11 mL, 0.11 mmol, 0.33 equiv, 1 M in DCM) were added to the flask then cooled to 0 ˚C for 10 minutes. 2,4,6-Collidine (0.10 mL, 0.69 mmol, 2.1 equiv) was added to the reaction mixture dropwise then stirred for 10 minutes at 0 ˚C. The reaction mixture was transferred to another flame-dried round bottom flask containing a magnetic stir bar and spiro[cyclopropane-1,2'-indolin]-3'-one (0.052 g, 0.33 mmol, 1.0 equiv) and stirred for 20 h at room temperature. The reaction mixture was quenched with sat. NH_4Cl, extracted with CH_2Cl_2 (3x), dried ($MgSO_4$), filtered and concentrated under reduced pressure. The crude product was purified using SiO_2 flash column (5-100% MeCN:H_2O with 0.1% formic acid) to yield 0.057 g (39%) of **21** as an orange oil; ^{1}H NMR (500 MHz, Chloroform-d) rotamers present and reported as observed: δ 7.83 (d, *J* = 7.4 Hz, 1H), 7.62 (m, 2H), 7.42 – 7.17 (m, 15H), 5.25 – 5.13 (m, 2H), 5.06 (t, *J* = 10.6 Hz, 1H), 4.10 (q, *J* = 7.1 Hz, 0.18H), 3.94 – 3.80 (m, 2H), 3.80 – 3.68 (m, 2H), 3.63 (t, *J* = 14.7 Hz, 1H), 3.56 (d, J = 3.3 Hz, 1H), 3.46 (d, *J* = 3.3 Hz, 0.15H), 3.43 – 3.28 (m, 0.13H), 3.28 – 3.11 (m, 0.29H), 2.97 (t, *J* = 6.7 Hz, 0.17H), 2.80 – 2.71 (m, 1H), 2.66 (t, *J* = 11.9 Hz, 1H), 2.56 – 2.38 (m, 1H), 2.31 (d, *J* = 24.8 Hz, 1H), 2.22 (t, *J* = 13.9 Hz, 2H), 2.12 (d, *J* = 10.9 Hz, 1H), 2.03 (d, *J* = 15.7 Hz, 2H), 1.98 – 1.88 (m, 1H), 1.84 (d, *J* = 8.7 Hz, 1H), 1.69 (m, 13H), 1.56 – 1.38 (m, 2H), 1.37 (s, 2H), 1.24 (d, *J* = 16.6 Hz, 1H), 0.92 (t, *J* = 7.4 Hz, 7H); ESIMS *m/z* 445.3 $[M+H]^+$.

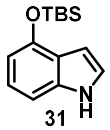

4-((tert-Butyldimethylsilyl)oxy)-1H-indole (31).[16] A round bottom flask and magnetic stir bar were flame-dried and placed under N_2 atmosphere. 4-hydroxyindole (1.00 g, 7.43 mmol, 1.0 equiv), DMF (12.7 mL, 22 equiv) imidazole (0.92 g, 13.38 mmol, 1.8 equiv), and *tert*-butyldimethylchlorosilane (1.26 mL, 8.18 mmol, 1.1 equiv) were added to the flask then stirred for 3 hours at room temperature. To the reaction mixture EtOAc and H_2O were added, and the organic layer was separated. The aqueous layer was extracted with EtOAc (3x) and the combined organic layers were dried ($NaSO_4$), filtered, and concentrated under

reduced pressure. The product was then dissolved in EtOAc and was washed with 5% LiCl (3x), dried ($NaSO_4$), filtered, and concentrated under reduced pressure. The product was used without purification to yield 1.58 g (86%) of **31** as a black solid. ^{1}H NMR (500 MHz, Chloroform-d) δ 8.10 (s, 1H), 7.12 – 7.08 (m, 1H), 7.05 – 6.98 (m, 1H), 6.61 – 6.56 (m, 1H), 6.52 (dd, *J* = 5.8, 2.6 Hz, 1H), 1.06 (s, 9H), 0.24 (s, 6H).

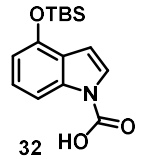

32

4-((tert-Butyldimethylsilyl)oxy)-1H-indole-1-carboxylic acid (32).[14] A round bottom flask and magnetic stir bar were flame-dried and placed under N_2 atmosphere. 4-((tert-butyldimethylsilyl)oxy)-1H-indole (1.58 g, 6.37 mmol, 1.0 equiv) and diethyl ether (31.9 mL, 0.2 M) were added to the flask then cooled to 0 ˚C. ^{n}BuLi (4.37 mL, 2.5 M in pentane, 1.2 equiv) was added to the reaction mixture dropwise at 0 ˚C. The reaction was refluxed for 2 hours then cooled to 0 ˚C. CO_2 was added to the reaction and bubbled for 30 mins. To the reaction mixture was quenched with H_2O, washed with H_2O, and the aqueous layer was acidified to pH 2. The formed precipitate was collected and dried under reduced pressure. The product was used without purification to yield 1.20 g (65%) of **32** as a gray solid. ^{1}H NMR (500 MHz, Chloroform-d) δ 7.83 (d, *J* = 8.2 Hz, 1H), 7.54 (d, *J* = 3.6 Hz, 1H), 7.21 (t, *J* = 8.1 Hz, 1H), 6.71 (d, *J* = 7.4 Hz, 2H), 1.05 (s, 9H), 0.24 (s, 6H); HRMS (ESI) *m/z* calculated for $C_{15}H_{21}NO_3Si$ $[M+H]^+$: 292.13635, found: 292.13721.

Chapter 2: Development of Metal Catalyzed Asymmetric Cyclopropanation

2.1 Introduction

Eburnamonine **3**, aspidospermidine **4**, and melokhanine E **5** are structurally complex molecules that contain a piperidine bearing a C3 all-carbon quaternary center moiety. This moiety is considered a privileged structure that exists in other biologically active natural products such as vinblastine (a chemotherapy drug), manzamine A, and an array of other bioactive alkaloids. This quaternary substituted piperidine represents a key synthetic challenge for efficient and scalable access to these families of natural products and this has been recognized by leading groups;[17–19] however, there remains a lack of stereoselective approaches that do not require many redox manipulations to access the target natural product cores. Therefore, there is a demand for a novel approach to install this stereocenter asymmetrically to access entire classes of natural products via more efficient and selective means. Herein, an investigation of an asymmetric cyclopropanation of a piperidine derived enecarbamate **19** to install the desired C3 all carbon quaternary center is explored.

In order to access the C3 stereocenter, **19** can be cyclopropanated via known methods utilizing Cu(I)OTf; however, no enantioselective version of this chemistry has been developed and the current approach provides both a mixture of enantiomers and diastereomers (**Scheme 10**).

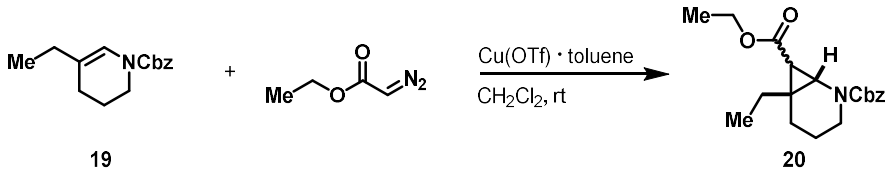

19 20

Scheme 10. Cu(I)OTf catalyzed cyclopropanation of enecarbamate.

Therefore, there is a need to develop a catalytic asymmetric cyclopropanation reaction. Once conditions are optimized, cyclopropane **20** is poised to undergo opening to access an array of natural product scaffolds without additional redox manipulations (**Scheme 11**). This transformation will be scaled up and incorporated in the synthesis of natural products in hopes to increase the yield and decrease the overall number of synthetic steps. The initial targets for this synthesis will be the first asymmetric synthesis of melokhanine E and bisleuconothines A and C.

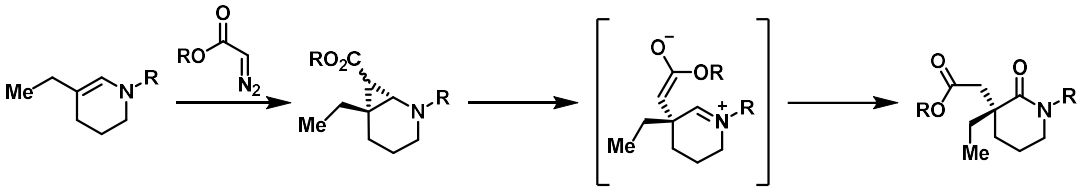

Scheme 11. C3 quaternary center piperidine synthesis via enantioselective cyclopropanation followed by cyclopropane ring opening.

2.2 Synthetic efforts

The enecarbamate was originally subjected to Cu(I)OTf paired with ethyl diazoacetate (EDA) cyclopropanation conditions for their ability to be modified with chiral ligands in hopes to promote enantioselectivity. The initial approach focused on utilizing commonly employed BOX ligands. BOX ligands are capable of distinguishing very similar diastereomeric transition states but have not yet been employed in systems such as those envisioned here (**Scheme 10**). For instance, the BOX ligands' varying substituents will affect the orientation the enecarbamate can approach and bind from because of the chiral environment that is formed (**Scheme 12**). This is done by the steric control of the ligand causing ideally only one appropriate orientation for the enecarbamate to approach to reduce the steric interactions and form the cyclopropane enantioselectively. Once the product is formed the copper-ligand complex can then dissociate and begin another catalytic cycle.

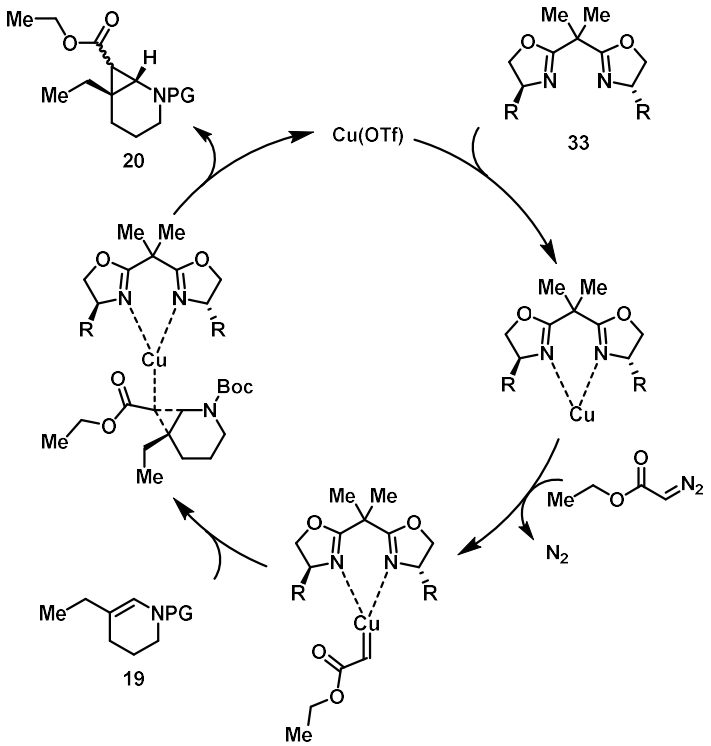

Scheme 12. Catalytic cycle of Cu(I)OTf-BOX ligand cyclopropanation.

The first attempts using a variety of commercially available BOX ligands were unsuccessful and no enantioselectivity was observed (**Figure 2**). Given this initial lack of success with BOX ligands, an alternative approach was selected, and aza-BOX ligands were the next target for exploration.

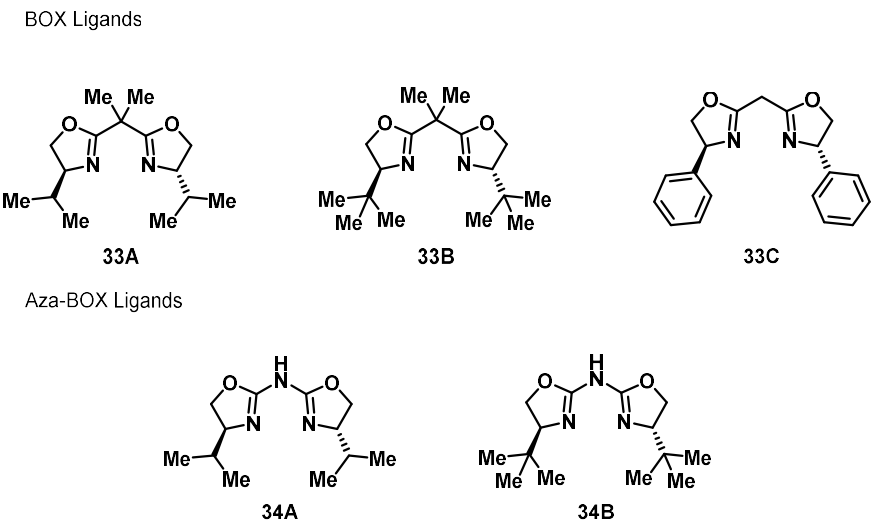

Figure 2. BOX ligands tested for enantioselectivity for enecarbamate cyclopropanation and potential aza-BOX ligands.

2.2.1 AzaBOX Ligand Synthesis

These azaBOX ligands **34** have been used to enantioselectively cyclopropanate alkenes such as pyrrole and furans.[20,21] These ligands are currently not commercially available so a synthesis by the Reiser group was followed.[22]

This method involves a simple substitution reaction between the amino-oxazoline **35** and ethoxyoxazoline **36** in the presence of a catalytic amount of *p*-toluenesulfonic acid (*p*-TsOH) to give the desired aza-BOX ligand **34** (**Scheme 13**).

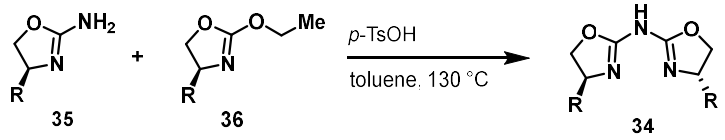

Scheme 13. Synthesis of aza-BOX ligands.

To synthesize the amino-oxazoline **35B**, an amino alcohol, in this case L-t*ert*-leucinol **37**, was cyclized with cyanogen bromide, generated from sodium cyanide and bromine (**Scheme 14**).

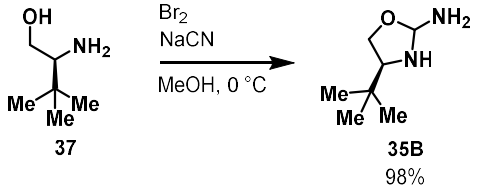

Scheme 14. Synthesis of amino-oxazoline.

The initial attempt to synthesis the ethoxyoxazoline coupling partner was successful (**Scheme 15**). Amino alcohol L-t*ert*-leucinol (**37**) was cyclized with diethyl carbonate and sodium ethoxy to afford the oxazolidone **39B**. The oxazolidone **39B** was then *O*-alkylated with triethyloxonium tetrafluoroborate (Et_3OBF_4) to afford the *tert*-butyl ethoxyoxazoline **36B**.

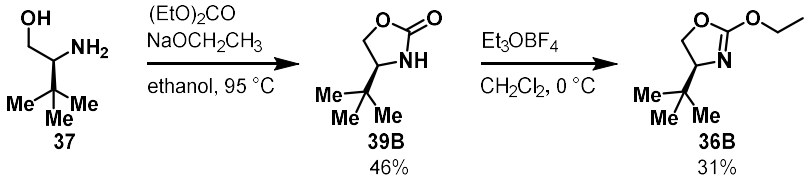

Scheme 15. Initials synthesis of tert-butyl ethoxyoxazoline.

With both coupling partners **35B** and **36B** in hand the *p*-toluenesulfonic acid (*p*-TsOH) catalyzed coupling was performed with no desired product observed (**Scheme 16**). Most likely to do the evaporation of solvent during the 24 h reflux.

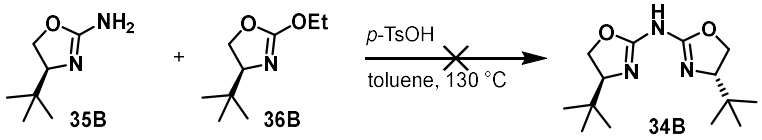

Scheme 16. Initial attempt at coupling amino-oxazoline **35B** and ethoxyoxazoline **36B**.

With the intention of reattempting the coupling more ethoxyoxazoline **36** needed to be made. However, this time the *O*-alkylation reaction was proving to be difficult to replicate (**Table 2**). When reattempting this transformation there was no conversion observed even when increasing the reaction time there was no improvement (**Table 2, entry 2-3**). When changing the method of addition of the triethyloxonium tetrafluoroborate (Et_3OBF_4) and the source there still was only a slight change in reactivity (**Table 2, entries 4-6**). After some literature searching it was noted in the experimental of Gawley and coworkers that commercially available solutions of Et_3OBF_4 were not recommended and the Et_3OBF_4 crystalline solid should be freshly prepared and properly stored before the reaction.[23]

Table 2. *O*-alkylation attempts

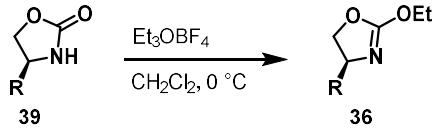

entry	R group	Et_3OBF_4[b]	time	yield
1	*t*-Bu	in DCM	overnight	31%
2	*t*-Bu	in DCM	overnight	no conv.
3[a]	*t*-Bu	in DCM	72 h	no conv.
4	*i*-prop	in DCM/slow addition	48 h	slight conv.
5	*i*-prop	in DCM/slow addition	24 h	slight conv.
6	*i*-prop	solid diluted with DCM[c]	overnight	slight conv.

[a]LCMS showed product mass but the product was not present by ^{1}H NMR, [b]commercially sourced, [c]prepared from commercial solid.

With continued difficulty synthesizing the ethoxyoxazolines **36**, a switch to the previous method for synthesizing these compounds reported by Reiser was made (**Scheme 17**).[22] This method only utilized the amino-oxazoline which then treated with benzaldehyde to perform a formal acid-catalyzed dimerization to form the desired aza-BOX ligand. The only drawback to this method was the difficulty of purification. However, Reiser et al. reported being able to successfully purify the *tert*-butyl and *iso*-propyl substituted aza-BOX ligands which are the current target compounds.

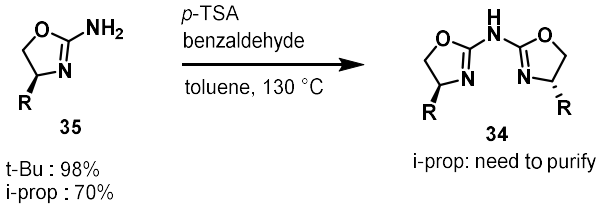

Scheme 17. Formal acid-catalyzed dimerization of amino-oxazoline.

Although two aza-BOX ligands are almost available for screening after purification there is still an interest in exploring chiral ligands that are already coordinated to the metal prior to starting the reaction. Cu(I)OTf is not air stable and degrades quickly when exposed to air making it cumbersome to work with without adequate equipment and techniques. Additionally, since we are using a different species and reaction set up then originally reported, there are variations in the observed reactivity. Looking at alternative, more robust, catalysts are of high interest to avoid the unforgiving nature of Cu(I)OTf.

2.2.2 Catalyst Screening

To begin the catalyst screening only catalysts that were currently in the inventory were selected (**Table 3**). This screening was performed in open air and without slow addition of the EDA, conditions critical for the success of the Cu(I)OTf reaction, to quickly observe potential reactivity. This explains the poor results for the standard Cu(I)OTf and surprisingly all of the tested catalysts yielded product via LCMS and NMR. This is especially exciting because of the success of rhodium, both well studied and readily availability from commercial sources.

Table 3. Preliminary catalyst screening for the cyclopropanation of enecarbamate.

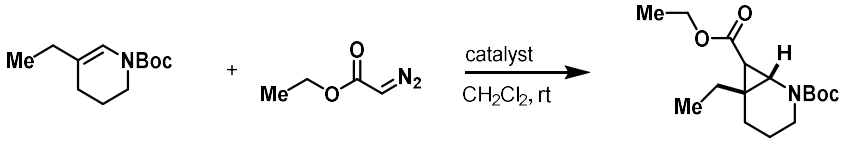

40 1 equiv. 41

entry	catalyst	result	diastereomer ratio[a]
1	CuOTf-toluene	product	poor resolution
2	Rh_2(*S*-PTAD)$_4$	product	(0.38:0.62)
3	$Cu(MeCN)_4BF_4$	product	(0.42:0.58)
4	$Rh_2(esp)_2$	product	(0.57:0.43)
5	$Rh_2(AcO)_4$	product	(0.50:0.50)
6	$Rh_2(CH_3(CH_2)_5CH_2CO_2)_4$	product	(0.43:0.57)
7	no cat.	no product	no product

[a]ratio between diastereomer peaks determined from ^{1}H NMR integration.

2.2.3 Optimization of Rhodium Acetate Cyclopropanation

Once Rhodium was identified as a catalyst for cyclopropanation of enecarbamate optimization studies were underway using Rhodium(II) acetate ($Rh_2(OAc)_4$). $Rh_2(OAc)_4$ was chosen for its relatively cheap price and commercial availability. The first condition to be optimized was the length of time the EDA was added over the course of the reaction and how long the reaction was left to run (**Table 4**). EDA is highly reactive and decomposes to form N_2 gas upon coordination to the metal center. However, the reaction is prone to dimerizing with itself if not enough starting material is able to interact with it in time. To combat this, the length of time to add the EDA to the reaction was lengthened to allow more time for the starting material to react with the coordinated EDA. When looking at the data overall it seems that as the addition time increases the yield increases. The reaction time was also evaluated by looking at the percent conversion immediately after the EDA addition verses 18 hours later. Theoretically, if all the EDA reacts upon addition

to the reaction and there isn't a need to run the reaction any longer. However, in the original reporting of the reaction with Cu(I)OTf the reaction ran for 18 h even after addition was complete. When comparing the data between the two aliquots there wasn't much of a difference in conversion between the two time points. This result indicated that it's not necessary to continue the reaction past the addition of EDA.

Table 4. EDA addition time and reaction time screening.

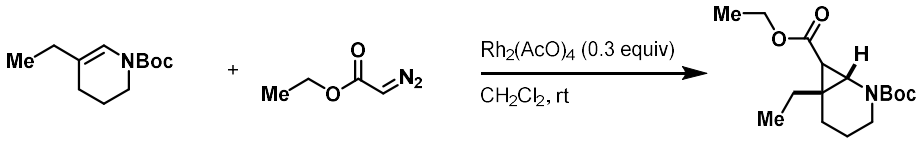

40 1 equiv. **41**

entry	addition time (min)	reaction time (h)	% conv.[a]
1[b]	0	0	8
2	0	18	11
3[c]	10	0	13
4[c]	10	18	14
5[c]	30	0	15
6[c]	30	18	16
7[c]	60	0	8
8[c]	60	18	11

[a]yield determined through ^{1}H NMR integration of crude reaction mixture, [b]average between multiple runs, [c]under Ar

The catalyst loading was then investigated to determine the effects of catalyst to the percent conversion (**Table 5**). When the catalyst loading was increased (**Table 5, entry 1**) the percent conversion went down potentially because of catalyst overloading the reaction and not disassociating properly for the reaction to continue the cycle. When the catalyst loading was lowered the percent conversion tended to increase. This was beneficial since lower catalyst loading was more cost effective.

Table 5. Catalyst loading.

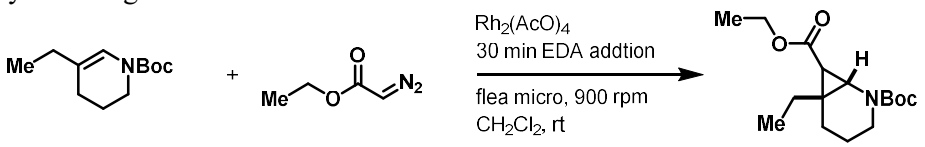

40 1 equiv. 41

entry	cat. loading (equiv)	% conv.[a]
1	0.4	20
2[b]	0.3	23
3	0.2	12
4	0.1	25
5	0.05	32
6	0.02	36

[a]yield determined through ^{1}H NMR integration of crude reaction mixture. [b]average between multiple runs.

Finally, the last parameter that was optimized was the amount of EDA added to the rection (**Table 6**). Since EDA dimerizes its common to add excess of this reagent in ensure full conversion of starting material to product. When increasing the EDA equivalents there was a clear increase in percent conversion. There were some underwhelming results when this set of experiment were run with 2 mol percent catalyst (**Table 6, entries 4-5**). This could be contributed to weighing errors of the catalyst since these experiments were performed on a small scale.

Table 6. EDA addition.

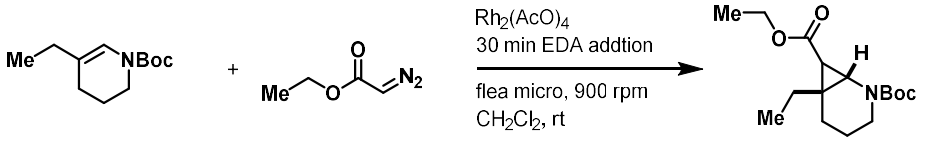

40 41

entry	cata. loading (equiv)	EDA (equiv)	% conv.[a]
1[b]	0.3	1	24
2	0.3	2	51
3	0.3	3	65
4[b]	0.02	1	23
5	0.02	2	26
6	0.02	3	35

[a]yield determined through integration of crude reaction mixture. [b]average between multiple runs.

A solvent screening was performed to determine any improvements to percent conversion, differences in dr, and alternative solvents for performing this transformation (**Table 7**). This initial screening only showed one solvent, 1,2-dichloroethane (DCE), as a potential alternative to methylene chloride (**Table 7, entry 2**). Dichloromethane will continue to be the main solvent for this transformation because of its abundance and availability.

Table 7. Solvent screening for Rh(I)acetate catalyzed cyclopropanation.

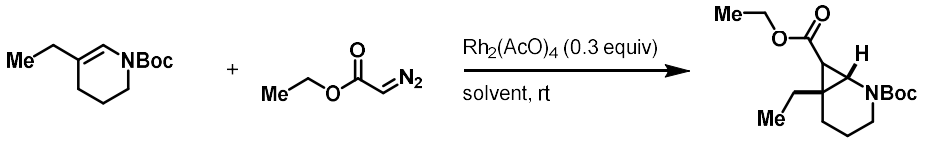

40 1 equiv. **41**

entry	solvent	result
1	methylene chloride	product
2	DCE	product
3	HFIP	no product
4	toluene	no product
5	THF	no product
6	*n*-heptane	no product
7	*n*-pentane	no product

With the newly optimized conditions in hand, it was now time to scale up these conditions from a 15 mg scale to a 300 mg scale. This large-scale reaction was performed with both 30 mol percent and 2 mol percent catalyst to determine if the reaction conditions were scalable and to see if the 2 mol percent was more reliable on a larger scale (**Scheme 13**). The EDA addition time was also increased to an hour to account for the larger scale. Both reactions resulted in full conversion of starting material to product. Making both conditions viable for this reaction.

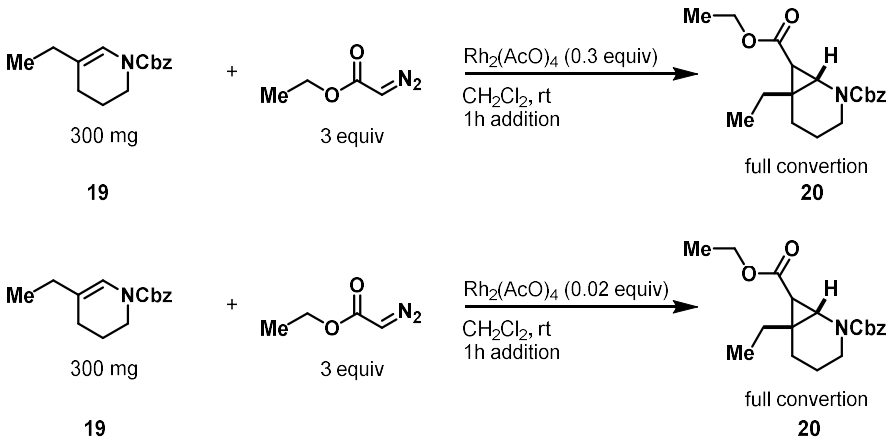

Scheme 18. Large scale Rh(I)acetate catalyzed cyclopropanation of enecarbamate.

With the reaction generally optimized, next was to get a yield using ^{1}H NMR and an internal standard (**Table 8**). After initial measurements showed surprisingly low yields the reactions were reoptimized using similar parameters to the initial optimization. However, there was little to no improvements in yield and the results were inconsistent. This indicated that similar to the Cu(II)OTf catalyst it also deals with issues of reproducibility.

Table 8. Re-optimization with ^{1}H NMR yields

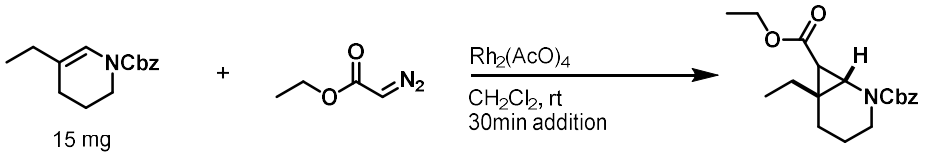

entry	cat. loading (eq)	EDA (eq)	NMR Yield[a]
1	0.4	3	17, 16
2	0.3	3	56, 22
3	0.2	3	13, 16
4	0.02	3	36, 11
5	0.01	3	0, 9
6	0.3	2	31
7	0.3	1	35
8	0.3	0.5	28

[a]Yields calculated using trimethoxybenzene internal standard.

2.4 Conclusions and Future Directions

Herein, I've reported the synthetic efforts towards a novel method to asymmetrically cyclopropanate enecarbamate to form the piperidine C3 all carbon quaternary center moiety found throughout many families of biologically active natural products. Some preliminary studies were performed utilizing BOX

ligands with no change to enantioselectivity. The synthesis of aza-BOX ligands are underway to further explore the possibility of modify the current Cu(II)OTf conditions to be asymmetric. A preliminary catalyst screening was performed to see find an alternative catalyst for this transformation and rhodium was identified as a potential candidate. Rhodium(II) acetate was used for optimization studies and although initial studies showed promising results the method suffered from reproducibility similar to the Cu(II)OTf conditions. Moving forward alternative metals and ligands will be investigated.

This method will enable enantioselective installation of the piperidine C3 all carbon quaternary center which will aid in the syntheses of new complex molecules and contribute to the growing interest in asymmetric catalysis. By implementing this reaction in already existing syntheses it could ease the overall synthesis by decreasing the number of synthetic steps and, as a result, increase the overall yields. This method will also help diversify existing natural products by allowing access to new analogs. Additionally, molecules that have yet to succumb to chemical synthesis, such as bisleuconothines A and C, will become accessible through these efforts.

2.5 Experimental

General: Dichloromethane were purified using an alumina filtration system and sparged before use. Starting materials were purchased from a commercial chemical company and used as received. Reactions were monitored by TLC analysis (pre-coated silica gel 60 F254 plates, 250 mm layer thickness) and visualization was accomplished with a 254 nm UV light and a silica iodine chamber. Reactions were also monitored by LC-MS (2.6 mm C18 50 x 2.10 mm column). Flash chromatography on SiO_2 was used to purify the crude reaction mixtures and performed on a flash system utilizing pre-packed cartridges and linear gradients. ^{1}H and ^{13}C NMR spectra were obtained on a 500 or 600 MHz instrument in $CDCl_3$ unless otherwise noted. Chemical shifts were reported in parts per million with the residual solvent peak used as an internal standard ($CDCl_3$ = 7.26 ppm for ^{1}H and 77.16 ppm for ^{13}C). ^{1}H NMR spectra were run at 500 or 600 MHz and are tabulated as follows: chemical shift, multiplicity (s = singlet, d = doublet, t = triplet, m = multiplet, bs = broad singlet, dd = doublet of doublets), number of protons, and coupling constant(s). ^{13}C NMR spectra were run at 125 MHz or 175 MHz using a proton-decoupled pulse sequence with a d1 of 1 second unless otherwise noted and are tabulated by observed peak. High-resolution mass spectra were obtained on an ion trap mass spectrometer using heated electrospray ionization (HESI).

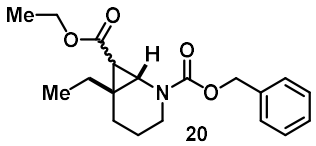

20

General procedure for 2-benzyl 7-ethyl (1S,6R)-6-ethyl-2-azabicyclo[4.1.0]heptane-2,7-dicarboxylate (41). A round bottom flask and magnetic stir bar were flame-dried and placed under atmosphere of N_2. The flask was charged with $Rh_2(OAc)_4$ (0.3 or 0.02 equiv), CH_2Cl_2 (1.0 M), and benzyl 5-ethyl-3,4-dihydropyridine-1(2H)-carboxylate (**19**) (1.0 equiv). Ethyl diazoacetate (3.0 equiv) was diluted with an equal part of CH_2Cl_2 then added to the flask via syringe pump over and hour. After completion, the reaction mixture was filtered through silica and concentrated under reduced pressure to yield the desired product (plus ethyl diazoacetate dimer) **20** as a clear, yellow oil.

Chapter 3: JAK/TRPV-1 Inhibitors

3.1 Introduction

Pain is unfortunately an inevitable response every living thing faces at some point in their lives, with chronic pain being one of the most severe forms. That is why it's important to develop methods to regulate this pain response and lessen their effects via pain relieving drugs.

Currently the most effective pain-relieving drugs on the market are opioids. Opioids such as morphine, oxycodone, and hydrocodone, although effective at relieving pain, are highly addictive. Despite their highly addictive nature they are still prescribed casually to treat minor/temporary pain problems resulting in 28% of the opioid overdose deaths in 2019.[24] This unfortunately can lead to a dangerous drug abuse cycle for users. Up to one-third of people who take opioids for chronic pain end up misusing them at some point and more than 10% get addicted to them over time.[25] These issues stemming from opioid use and mishandling, and the addictions that follow are dubbed the Opioid Epidemic. Because of the Opioid Epidemic there is now a great need for alternative methods of pain relief.

Opioids are used to mediate pain by targeting the opioid receptors. However, there are other receptors that can be triggered to mediate pain that aren't these highly addictive opioid receptors. Receptors such as the Janus kinases (JAK) and Transient Receptor Potential Vanilloid 1 (TRPV1) are primary candidates for alternative pain management pathways as there are currently drugs on the market that target these two pathways.

3.1.1 JAK inhibitors

Recently a few JAK inhibitors were approved by the Food and Drug Administration (FDA) to be used commercially (**Figure 3**).[26] To name a few, tofacitnib is used to treat rheumatoid arthritis and is used as a topical treatment to relieve the symptoms of rashes caused by psoriasis and atopic dermatitis. Ruxolitinib is used to treat blood and bone marrow cancers such as polycythemia and myelofibrosis. Finally, oclacitinib is used for canines to treat itch and lesions associated with atopic dermatitis.

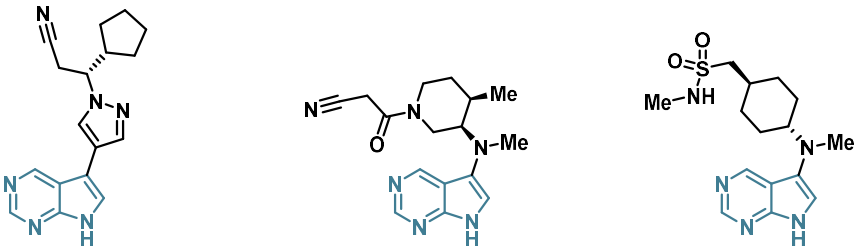

Figure 3. Current FDA approved JAK inhibitors.

3.1.2 TRPV1 inhibitors

TRPV1 inhibitors have also had some FDA approved drugs on the market (**Figure 4**). Most recognizable being capsaicin which, when used topically, has been found to have modest effects on patients suffering from chronic pain caused by osteoarthritis.[27] Another example is resiniferatoxin which was found to reduce joint pain.[28]

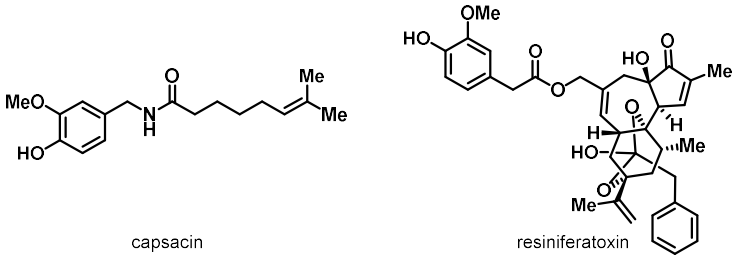

Figure 4. TRPV1 Inhibitors

Novel strategies such as JAK and TRPV1 inhibitors have shown to hold promise as alternatives to opioid therapeutics for pain management. These pathways allow for the modulation of pain through an alternative mechanism than that of opioids and are enticing drug candidates to combat the Opioid Epidemic.

3.2 Synthetic efforts

In 2017, Bäumer and coworkers reported a decrease in pain caused by itch using JAK inhibitors, tofacitinib and oclacitinib, and this decrease was attributed to these compounds also targeting TRPV1 receptors.[29] These results indicated a potential to develop an inhibitor that can target both the JAK and TRPV1 pathways when administered, equating to a more effective pain relief. To further understand this phenomenon Fourches and coworkers performed a molecular docking analysis to observe the probability of tofacitinib and oclacitinib binding to the capsaicin binding site. From these results potential JAK/TRPV1 inhibitors were modeled to maximize the inhibition of the TRPV1 pathway while also retaining the JAK inhibitory potential. From this, two classes of novel JAK/TRPV1 inhibitors emerged which possessed a

2,4-disubstituted pyrimidine (pyrimidine analogs) and a 3-substituted 7-azaindole (7-azaindole analogs) scaffold (**Figure 5**).

Figure 5. Potential dual JAK/TRPV1 inhibitors

Since these potential inhibitors have been identified there has been a library of 27 compounds synthesized to test for their ability to be dual JAK/TRPV1 inhibitors (**Figure 6**). Each compound was subjected to separate phenotypic JAK and TRPV1 assays that measured the cytokine secretion in dendritic cells via the inhibition of the respective pathways.[30] Compounds that inhibited cytokine secretion were labeled (+) and some assays were performed more than once.

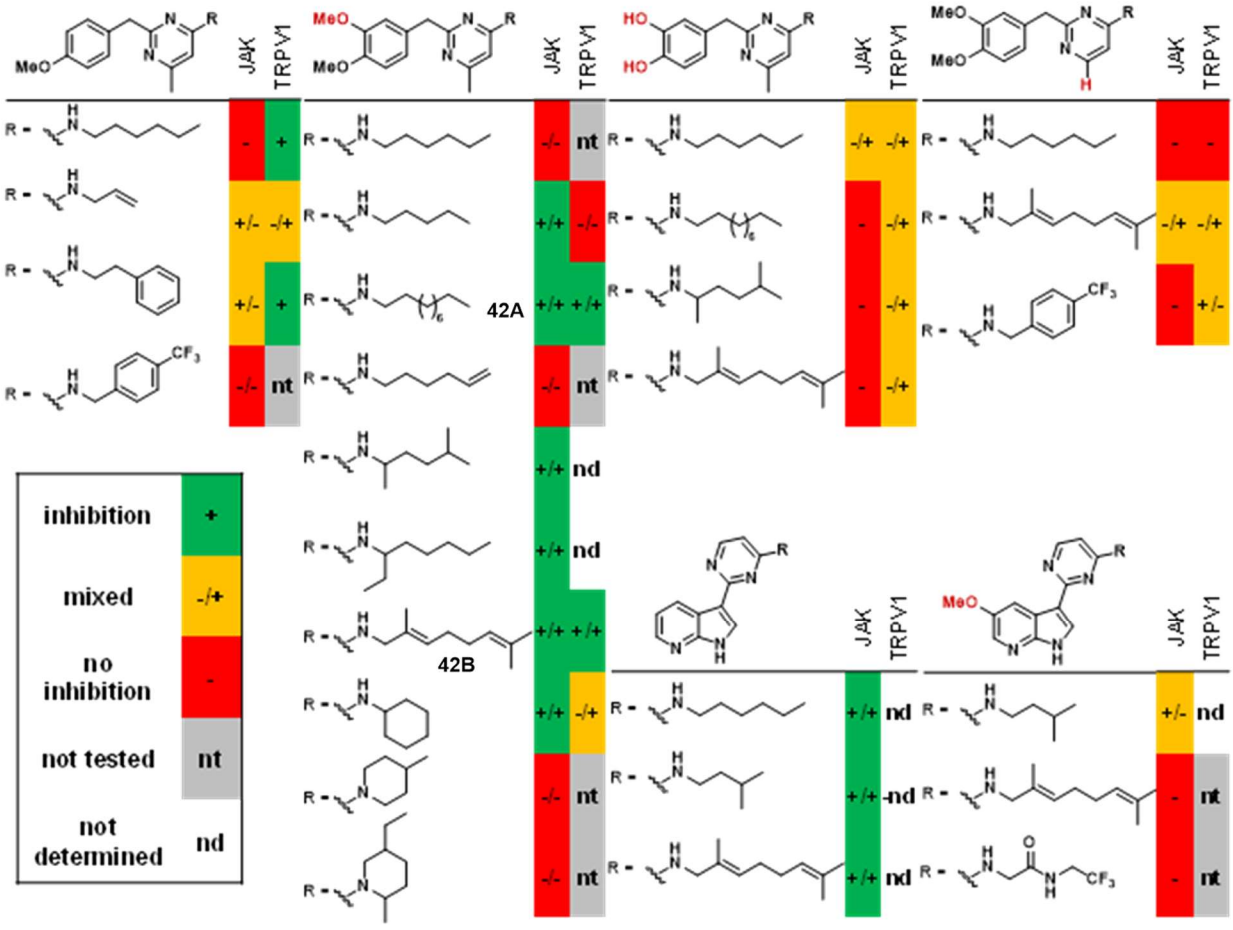

Figure 6. Library of potential JAK/TRPV1 inhibitor and their response to JAK and TRPV1 assays.

From these assays two potential dual inhibitors **42A** and **42B** were identified due to their duplicate positive test results in both the JAK and TRPV1 assays. Although there is still an interest in the unsubstituted azaindole inhibitors as they haven't been subjected to the TRPV1 assay and show promising results from the JAK assay.

Also, an alternative pyrimidine analog with a similar structure to capsaicin is of interest to synthesize and test (**Scheme 19**). As the presence of both a methoxy and alcohol substituent may yield stronger bonding and higher reactivity.

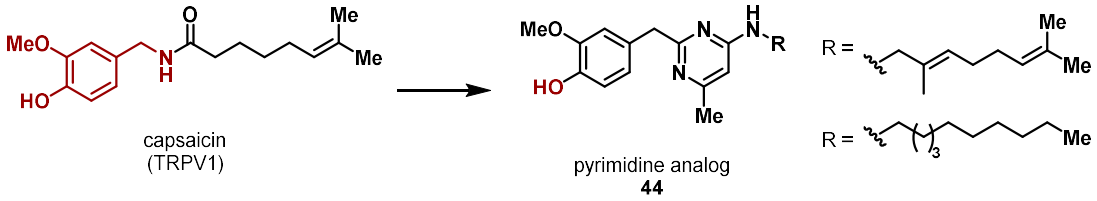

Scheme 19. Capsaicin inspired pyrimidine analog.

3.2.1 Pyrimidine analog synthesis

Since there were two promising dual JAK/TRPV1 inhibitors identified from the preliminary data, **42A** and **42B**, it was important to remake these compounds to confirm their reactivity and to further explore their mode of action. To access these analogs 2-phenylacetonitrile **45** was treated with trimethyl aluminum to access the guanidinium intermediate **46** (**Scheme 20**). The guanidinium was then condensed with ethyl acetoacetate to yield the pyrimidone **47**. The pyrimidone **47** was then refluxed in freshly distilled phosphorous oxychloride ($POCl_3$) to give the chloro-substituted pyrimidine **48**. Finally, the chloro-substituted pyrimidine **48** was treated with various amine nucleophiles to yield the desired pyrimidine analogs **42A** and **42B**.

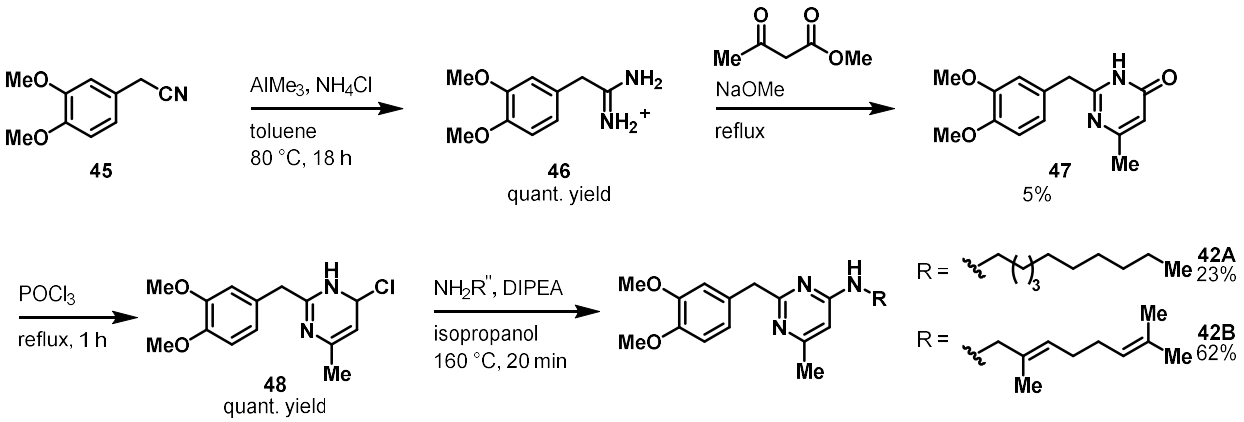

Scheme 20. Synthesis of a pyrimidine analog JAK/TRPV1 inhibitor.

To access the new capsaicin inspired pyrimidine analog **44**, vanillin (**49**) was allyl protected using allyl bromide and potassium carbonate to yield **50** (**Scheme 21**). The protected vanillin was then treated with

toluenesulfonylmethyl isocyanide (TosMIC) then methanol (MeOH) to transform the aldehyde to the nitrile **51**. Form here the original synthesis is performed up until the amine addition. From here a deprotection will take place to yield the desired capsaicin inspired pyrimidine analog **44**.

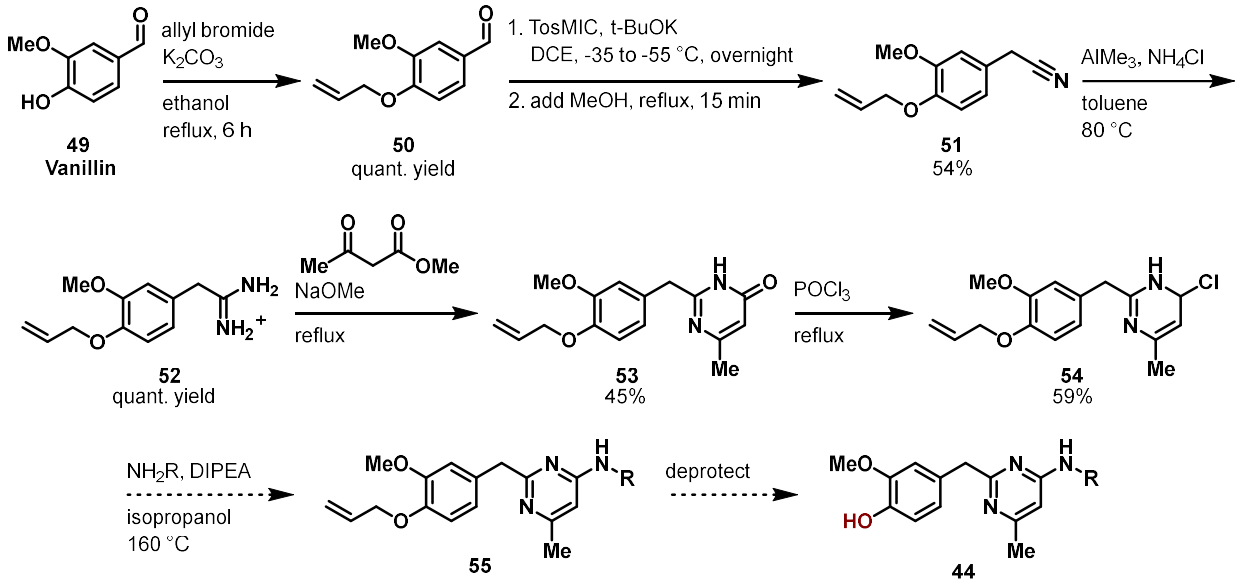

Scheme 21. Synthesis of capsaicin inspired pyrimidine analog.

3.2.2 7-Azaindole analog synthesis

The preliminary data gathered for the azaindole analogs were promising for the unsubstituted azaindole **43** as JAK inhibitors but still needed further testing to see if they inhibit the TRPV1 pathway. There is still an interest in exploring the dual inhibition potential so additional analogs are being made for further testing.

To synthesize these analogs, 7-azaindole **56** was brominated using *N*-bromosuccinimide (NBS) to yield 3-bromo-7-azaindole **57** (**Scheme 22**). The brominated intermediate **57** was then protected with 4-toulenesulfonylchloride (TsCl) to give the tosyl-protected azaindole **58**. The protected azaindole **58** was then treated with bis(pinacolato)diboron (B_2pin_2) and palladium tetrakis(triphenylphosphine) to yield the boronate **59** which is the first Suzuki coupling partner.

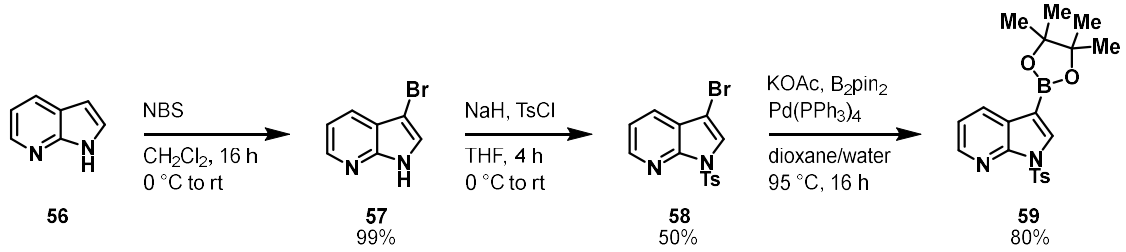

Scheme 22. Synthesis of tosyl-protected 7-azaindole boronate.

To access the other Suzuki coupling partner **61**, 2,4-dichloropyrimidine was treated with various amine nucleophiles and Hunig's base (**Scheme 23**).

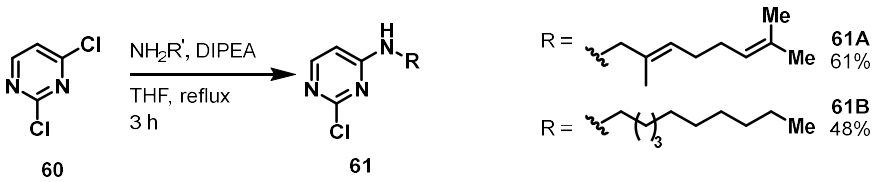

Scheme 23. Synthesis of amine substituted 2-dichloropyrimidine.

With both coupling partners in hand a Suzuki coupling was performed using palladium(0) tetrakis(triphenylphosphine) $Pd(PPh_3)_4$ to form the protected azaindole analog (**Scheme 24**). Finally, the azaindole analog was deprotected using potassium carbonate to yield the desired azaindole analog **43A** and a new analog **43B**.

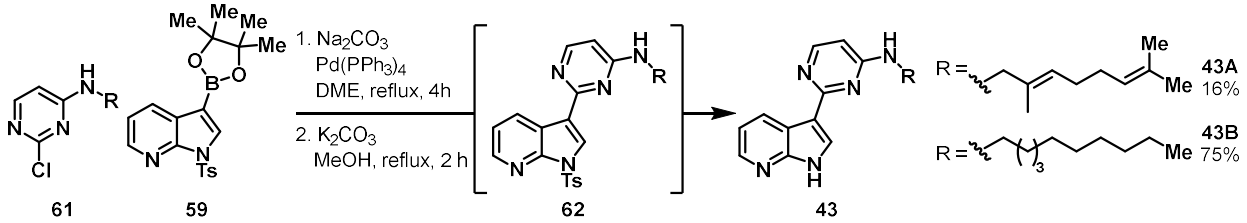

Scheme 24. Suzuki Coupling and Deprotection to form the Azaindole Analog JAK/TRPV1 Inhibitors.

3.3 Conclusion and Future Directions

Herein, I have reported by progress towards the synthesis of potential dual JAK/TRPV1 inhibitors. Of the four currently synthesized, one is a novel untested 7-azaindole inhibitor. The progress towards the synthesis of a capsaicin inspired pyrimidine analog was reported. The currently synthesized compounds and future compounds will be sent to collaborations for the testing of their biological activity.

3.4 Experimental

General: THF and dichloromethane were purified using an alumina filtration system. Starting materials were purchased from a commercial chemical company and used as received. Reactions were monitored by TLC analysis (pre-coated silica gel 60 F254 plates, 250 mm layer thickness) and visualization was accomplished with a 254 nm UV light and silica iodine chamber. Reactions were also monitored by LC-MS (2.6 mm C18 50 x 2.10 mm column. Flash chromatography on SiO_2 was used to purify the crude reaction mixtures and performed on a flash system utilizing pre-packed cartridges and linear gradients. ^1H and ^{13}C NMR spectra were obtained on a 500 or 600 MHz instrument in $CDCl_3$ or acetone-d_6 unless otherwise noted. Chemical shifts were reported in parts per million with the residual solvent peak used as an internal standard ($CDCl_3$ = 7.26 ppm for ^1H and 77.16 ppm for ^{13}C, acetone-d_6 = 2.05 ppm for ^1H and

29.84 ppm for ^{13}C NMR). ^{1}H NMR spectra were run at 500 or 600 MHz and are tabulated as follows: chemical shift, multiplicity (s = singlet, d = doublet, t = triplet, m = multiplet, bs = broad singlet, dd = doublet of doublets), number of protons, and coupling constant(s). ^{13}C NMR spectra were run at, 125 MHz or 175 MHz using a proton-decoupled pulse sequence with a d1 of 1 second unless otherwise noted and are tabulated by observed peak. High-resolution mass spectra were obtained on an ion trap mass spectrometer using heated electrospray ionization (HESI).

Compounds **42**-**43**, **46**-**48**, **57**-**62** were prepared by known literature methods.[31]

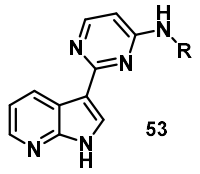

53

General procedure for Compound (4-25)[31] To a solution of **59** (0.1 g, 0.25 mmol) in DME (0.2 M) and water (0.08 M) was added **61** (0.05 g, 0.28 mmol) and Na_2CO_3 (0.08 g, 0.75 mmol). The resulting solution was degassed using argon. Then, $Pd(PPh_3)_4$ (0.03 g, 0.03 mmol) was added, and the resulting mixture was heated to reflux for 16 h, cooled to room temperature, filtered over Celite, then florisil. The filtrate was washed with 15 mL EtOAc, and the filtrate was concentrated in vacuo to yield **62**. The crude product **62** was redissolved in MeOH (0.1 M), and K_2CO_3 (0.069 g, 0.50 mmol) was added. The resulting solution was refluxed for 3 h, cooled to room temperature, and the solvent evaporated. The crude mixture was purified using SiO_2 flash column (5-100% MeOHn:DCM) to yield **53** as an oil.

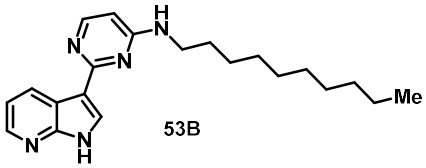

53B

***N*-decyl-2-(1H-pyrrolo[2,3-b]pyridin-3-yl)pyrimidin-4-amine (53B).** Yield 67 mg (75%) as brown oil. ^{1}H NMR (600 MHz, Acetone-d_6) δ 10.78 (s, 1H), 8.04 – 7.90 (m, 1H), 7.75 – 7.67 (m, 2H), 7.64 – 7.58 (m, 1H), 7.54 – 7.45 (m, 2H), 5.94 (d, J = 5.6 Hz, 1H), 3.39 (m, 2H), 1.62 (p, J = 7.1 Hz, 2H), 1.37 – 1.21 (m, 14H), 0.87 (t, J = 6.9 Hz, 3H); ^{13}C NMR (151 MHz, Acetone-d_6) δ 163.85, 159.08, 148.48, 143.64, 128.80, 121.52, 120.86, 116.41, 101.62, 101.00, 53.00, 41.91, 32.63, 27.73, 23.32, 14.36; ESIMS *m/z* 352.3 $[M+H]^+$.

References

(1) Understanding What Cancer Is: Ancient Times to Present https://www.cancer.org/cancer/cancer-basics/history-of-cancer/what-is-cancer.html (accessed 2022 -04 -14).

(2) CDC. Cancer Data and Statistics https://www.cdc.gov/cancer/dcpc/data/index.html (accessed 2022 -04 -14).

(3) Huang, M.; Lu, J.-J.; Ding, J. Natural Products in Cancer Therapy: Past, Present and Future. *Nat. Prod. Bioprospecting.* **2021**, *11* (1), 5–13.

(4) Koehn F. E. Natural Products and Cancer Drug Discovery. Springer, 2013.

(5) Nugroho, A. E.; Zhang, W.; Hirasawa, Y.; Tang, Y.; Wong, C. P.; Kaneda, T.; Hadi, A. H. A.; Morita, H. Bisleuconothines B–D, Modified Eburnane–Aspidosperma Bisindole Alkaloids from Leuconotis Griffithii. *J. Nat. Prod.* **2018**, *81* (11), 2600–2604.

(6) Hirasawa, Y.; Shoji, T.; Arai, T.; Nugroho, A. E.; Deguchi, J.; Hosoya, T.; Uchiyama, N.; Goda, Y.; Awang, K.; Hadi, A. H. A.; Shiro, M.; Morita, H. Bisleuconothine A, an Eburnane–Aspidosperma Bisindole Alkaloid from Leuconotis Griffithii. *Bioorg. Med. Chem. Lett.* **2010**, *20* (6), 2021–2024.

(7) Wong, C. P.; Seki, A.; Horiguchi, K.; Shoji, T.; Arai, T.; Nugroho, A. E.; Hirasawa, Y.; Sato, F.; Kaneda, T.; Morita, H. Bisleuconothine A Induces Autophagosome Formation by Interfering with AKT-MTOR Signaling Pathway. *J. Nat. Prod.* **2015**, *78* (7), 1656–1662.

(8) Li, G.; Piemontesi, C.; Wang, Q.; Zhu, J. Stereoselective Total Synthesis of Eburnane-Type Alkaloids Enabled by Conformation-Directed Cyclization and Rearrangement. *Angewandte. Chemie. Int. Ed.* **2019**, *58* (9), 2870–2874.

(9) Cheng, G.-G.; Li, D.; Hou, B.; Li, X.-N.; Liu, L.; Chen, Y.-Y.; Lunga, P.-K.; Khan, A.; Liu, Y.-P.; Zuo, Z.-L.; Luo, X.-D. Melokhanines A–J, Bioactive Monoterpenoid Indole Alkaloids with Diverse Skeletons FromMelodinus Khasianus. *J. Nat. Prod.* **2016**, *79* (9), 2158–2166.

(10) Xu, H.; Huang, H.; Zhao, C.; Song, C.; Chang, J. Total Synthesis of (+)-Aspidospermidine. *Org. Lett.* **2019**, *21* (16), 6457–6460.

(11) Cholewczynski, A. E.; Williams, P. C.; Pierce, J. G. Stereocontrolled Synthesis of (±)-Melokhanine E via an Intramolecular Formal [3 + 2] Cycloaddition. *Org. Lett.* **2020**, *22* (2), 714–717.

(12) Wenkert, E.; Hudlicky, T. Synthesis of Eburnamonine and Dehydroaspidospermidine. *J. Org. Chem.* **1988**, *53* (9), 1953–1957.

(13) Pandey, G.; Mishra, A.; Khamrai, J. Asymmetric Total Synthesis of Eburnamine and Eucophylline: A Biomimetic Attempt for the Total Synthesis of Leucophyllidine. *Org. Lett.* **2017**, *19* (12), 3267–3270.

(14) De Simone, F.; Gertsch, J.; Waser, J. Catalytic Selective Cyclizations of Aminocyclopropanes: Formal Synthesis of Aspidospermidine and Total Synthesis of Goniomitine. *Angewandte. Chemie. Int. Ed.* **2010**, *49* (33), 5767–5770.

(15) Kawada, M.; Kawano, Y.; Sugihara, H.; TAKEI, S.; Imada, I. Spirocyclopropane Compounds. I. Synthesis and Reactivity of Spiro [Cyclopropane-1, 2'-[2H] Indol]-3'(1'H)-Ones. *Chem. Pharm. Bulletin.* **1981**, *29* (7), 1900–1911.

(16) Lu, B.; Falck, J. R. Efficient Iridium-Catalyzed C□H Functionalization/Silylation of Heteroarenes. *Angewandte. Chemie. Int. Ed.* **2008**, *47* (39), 7508–7510.

(17) Behenna, D. C.; Liu, Y.; Yurino, T.; Kim, J.; White, D. E.; Virgil, S. C.; Stoltz, B. M. Enantioselective Construction of Quaternary N-Heterocycles by Palladium-Catalysed Decarboxylative Allylic Alkylation of Lactams. *Nat. Chem.* **2012**, *4* (2), 130.

(18) Numajiri, Y.; Pritchett, B. P.; Chiyoda, K.; Stoltz, B. M. Enantioselective Synthesis of A-Quaternary Mannich Adducts by Palladium-Catalyzed Allylic Alkylation: Total Synthesis of (+)-Sibirinine. *J. Am. Chem. Soc.* **2015**, *137* (3), 1040–1043.

(19) Pritchett, B. P.; Kikuchi, J.; Numajiri, Y.; Stoltz, B. M. Enantioselective Pd-Catalyzed Allylic Alkylation Reactions of Dihydropyrido[1,2-a]Indolone Substrates: Efficient Syntheses of (−)-Goniomitine, (+)-Aspidospermidine, and (−)-Quebrachamine. *Angewandte. Chemie. Int. Ed.* **2016**, *55* (43), 13529–13532.

(20) Pilsl, L. K. A.; Ertl, T.; Reiser, O. Enantioselective Three-Step Synthesis of Homo-β-Proline: A Donor–Acceptor Cyclopropane as Key Intermediate. *Org. Lett.* **2017**, *19* (10), 2754–2757.

(21) Schinnerl, M.; Böhm, C.; Seitz, M.; Reiser, O. New Bis(Oxazoline) Ligands with Secondary Binding Sites for the Asymmetric Cyclopropanation of Furans. *Tetrahedron Asymmetry.* **2003**, *14* (7), 765–771.

(22) Werner, H.; Vicha, R.; Gissibl, A.; Reiser, O. Improved Synthesis of Aza-Bis(Oxazoline) Ligands. *J. Org. Chem.* **2003**, *68* (26), 10166–10168.

(23) Rein, K.; Goicoechea-Pappas, M.; Anklekar, T. V.; Hart, G. C.; Smith, G. A.; Gawley, R. E. Chiral Dipole-Stabilized Anions: Experiment and Theory in Benzylic and Allylic Systems. Stereoselective Deprotonations, Pyramidal Inversions, and Stereoselective Alkylations of Lithiated (Tetrahydroisoquinolyl)Oxazolines. *J. Am. Chem. Soc.* **1989**, *111* (6), 2211–2217.

(24) CDC. Prescription Opioid Overdose Death Maps https://www.cdc.gov/drugoverdose/deaths/prescription/maps.html (accessed 2022 -04 -14).

(25) NIH. Opioid Overdose Crisis https://nida.nih.gov/drug-topics/opioids/opioid-overdose-crisis (accessed 2022 -04 -14).

(26) O'Shea, J. J.; Schwartz, D. M.; Villarino, A. V.; Gadina, M.; McInnes, I. B.; Laurence, A. The JAK-STAT Pathway: Impact on Human Disease and Therapeutic Intervention*. *Annu. Rev. Med.* **2015**, *66* (1), 311–328.

(27) Guedes, V.; Castro, J. P.; Brito, I. Topical Capsaicin for Pain in Osteoarthritis: A Literature Review. *Reumatología Clínica.* **2018**, *14* (1), 40–45.

(28) Kissin, E. Y.; Freitas, C. F.; Kissin, I. The Effects of Intraarticular Resiniferatoxin in Experimental Knee-Joint Arthritis. *Anesthesia Analgesia.* **2005**, *101* (5), 1433–1439.

(29) Fukuyama, T.; Ganchingco, J. R.; Mishra, S. K.; Olivry, T.; Rzagalinski, I.; Volmer, D. A.; Bäumer, W. Janus Kinase Inhibitors Display Broad Anti-Itch Properties: A Possible Link through the TRPV1 Receptor. *J. Allergy. Clin. Immun.* **2017**, *140* (1), 306-309.

(30) Lutz, M. B.; Kukutsch, N.; Ogilvie, A. L. J.; Rößner, S.; Koch, F.; Romani, N.; Schuler, G. An Advanced Culture Method for Generating Large Quantities of Highly Pure Dendritic Cells from Mouse Bone Marrow. *J. Immunol. Methods.* **1999**, *223* (1), 77–92.

(31) Robinson, K. R. Synthesis and Biological Evaluation of 4-Oxazolidinones and Dual JAK/TRPV-1 Inhibitors. Ph. D. North Carolina State University, Raleigh, NC, 2020.